

# LoGSAM: Parameter-Efficient Cross-Modal Grounding for MRI Segmentation

Mohammad Robaitul Islam Bhuiyan<sup>1</sup>, Sheethal Bhat<sup>1,2</sup>, Melika Qahqaie<sup>1,2</sup>,  
Tri-Thien Nguyen<sup>1</sup>, Paula Andrea Pérez Toro<sup>1</sup>, Tomas Arias Vergara<sup>1</sup>, and  
Andreas Maier<sup>1</sup>

<sup>1</sup> Pattern Recognition Lab, Friedrich-Alexander-Universität, Erlangen, Germany

<sup>2</sup> Siemens Healthineers, Erlangen, Germany

mohammad.ri.bhuiyan@fau.de

**Abstract.** Precise localization and delineation of brain tumors using Magnetic Resonance Imaging (MRI) are essential for planning therapy and guiding surgical decisions. However, most existing approaches rely on task-specific supervised models and are constrained by the limited availability of annotated data. To address this, we propose LoGSAM, a parameter-efficient, detection-driven framework that transforms radiologist dictation into text prompts for foundation-model-based localization and segmentation. Radiologist speech is first transcribed and translated using a pretrained Whisper ASR model, followed by negation-aware clinical NLP to extract tumor-specific textual prompts. These prompts guide text-conditioned tumor localization via a LoRA-adapted vision-language detection model, Grounding DINO (GDINO). The LoRA adaptation updates using <5% of the model parameters, thereby enabling computationally efficient domain adaptation while preserving pretrained cross-modal knowledge. The predicted bounding boxes are used as prompts for MedSAM to generate pixel-level tumor masks without any additional fine-tuning. Conditioning the frozen MedSAM on LoGSAM-derived priors yields a state-of-the-art dice score of 80.32% on BRISC 2025. In addition, we evaluate the full pipeline using German dictations from a board-certified radiologist on 12 unseen MRI scans, achieving 91.7% case-level accuracy. These results highlight the feasibility of constructing a modular, speech-to-segmentation pipeline by intelligently leveraging pretrained foundation models with minimal parameter updates. The source code is at: <https://github.com/robayet002/LoGSAM>

**Keywords:** MRI Segmentation · LoRA-adapted Vision-Language detection · Foundation models

## 1 Introduction

Brain tumors such as gliomas, meningiomas, and pituitary tumors represent serious pathologies that can impact the central nervous system and require precise characterization for treatment planning [7]. Towards this end, contrast-enhanced T1-weighted Magnetic Resonance Imaging (MRI) is a popular imaging modality

used to identify active tumor regions [8]. Although MRI provides extensive diagnostic information, manual tumor delineation is time-consuming and depends on radiologist expertise [13]. Consequently, there is growing interest in automatic tumor segmentation methods. Despite recent advances, state-of-the-art (SOTA) segmentation algorithms require large datasets with dense pixel-level annotations. These are labor-intensive and expensive to collect in real life [2]. Moreover, in routine clinical workflows, radiologists typically dictate reports, which can be used as additional supervisory signals. However, due to ambiguity, variability, and negation in clinical language, naive keyword matching might lead to increased false positives [11,18]. To address these gaps, we propose a parameter-efficient speech-to-segmentation framework that transforms radiologist dictations into structured prompts for tumor localization and segmentation. This enables effective tumor delineation with minimal task-specific fine-tuning and improved robustness to unseen data distributions.

Recent advances in foundation models and vision–language learning offer an effective and scalable approach to fully supervised medical segmentation. In speech, the availability of high-accuracy automatic speech recognition (ASR) systems enables reliable transcription of multilingual radiologist dictations, making speech-derived supervision increasingly practical in clinical workflows [3]. Conversely, in the vision-language domain, clinical reports and textual cues have been successfully leveraged as weak supervisory signals for representation learning [14,15]. Furthermore, grounding-based approaches connect textual phrases to image regions, enabling text-conditioned localization [1]. In parallel, prompt-based segmentation frameworks such as the Segment Anything Model (SAM) and its medical adaptation MedSAM have demonstrated strong generalization across modalities when provided with appropriate prompts [17,4]. However, adapting large vision–language and segmentation models to specific medical domains remains computationally expensive. Parameter-efficient fine-tuning (PEFT) methods, such as LoRA, enable targeted adaptation while keeping most parameters frozen [6]. Recent works combining LoRA-based grounding with SAM-style segmentation suggest that detection-driven prompting can effectively guide segmentation in specialized domains [12,5].

Building upon these advances, a parameter-efficient, detection-driven speech-to-segmentation framework for brain tumor analysis. Radiologist dictations are transcribed [3] and converted into structured tumor prompts using negation-aware NLP [19], which guides text-conditioned localization via a LoRA-adapted grounding model. The resulting bounding boxes condition a prompt-based segmentation model to produce pixel-level masks without additional fine-tuning. By coordinating pretrained foundation models end-to-end, LoGSAM reduces reliance on dense annotations while maintaining robustness to unseen data.

**Main Contributions:** 1) We formulate speech-to-segmentation as a detection-driven, prompt-based learning paradigm that integrates automatic speech recognition, clinical NLP, grounding models, and medical segmentation within a unified, parameter-efficient framework. 2) We introduce a LoRA-based adaptation

strategy for text-conditioned grounding in brain MRI and systematically analyze its impact through ablations on rank selection and injection location. 3) We demonstrate robust generalization across datasets through out-of-distribution evaluation on 554 Kaggle MRI cases [21] and radiologist-guided testing with 12 German dictations, highlighting the practical applicability of the proposed speech-to-segmentation pipeline.

## 2 Method

### 2.1 Datasets

This study uses two datasets. BRISC includes 6,000 contrast-enhanced T1-weighted 2D MRI scans across four categories—*Glioma*, *Meningioma*, *Pituitary*, and *Healthy*—covering multiple anatomical planes (axial, coronal, and sagittal). All the images are in JPEG format with  $512 \times 512$  resolution, carefully curated, labeled, and quality-checked by radiologists and physicians. The images are collected from multiple public datasets that lack comprehensive acquisition metadata such as patients, slices, scanner type, or sequence parameter [20]. The dataset is mildly imbalanced, with pituitary (29.28%) and meningioma (27.25%), followed by glioma (23.35%) and healthy (20.12%). The dataset is split into 4000 (train), 1000 (val), and 1000 (test) images and is manually reviewed to minimize the risk of patient overlap between the training and test datasets.

As an out-of-distribution (OOD) dataset, we use the Kaggle *MRI for Brain Tumor with Bounding Box* [21], consisting of 5,249 JPEG images (glioma: 1289, meningioma: 1589, pituitary: 1560, healthy: 811). The annotations were created with the *LabelImg* tool in YOLO format, with most images labeled at a resolution of  $512 \times 512$ . The dataset is split into 3790 (train), 947 (val), and 509 (test) images. No information on the patients’ numbers, slices, or scanner type is available.

For evaluation, we use real German-language speech recordings dictated by a board-certified radiologist for 12 BRISC cases (three per class).

### 2.2 LoGSAM Pipeline

As illustrated in Fig. 1, the proposed pipeline has three main components: (i) a speech-to-prompt generation module, (ii) a LoRA-augmented GDINO model for text-conditioned tumor localization, and (iii) a prompt-based segmentation model based on MedSAM.

**Speech-to-prompt generation:** The input to this module is a board-certified radiologist’s dictated report, provided as an audio signal  $s(t)$ . The speech-to-prompt pipeline transforms this signal into a structured tumor prompt through the following processing chain:

$$s(t) \xrightarrow{f_{\text{ASR}}} y \xrightarrow{f_{\text{NLP}}} (c, n) \xrightarrow{g} p,$$

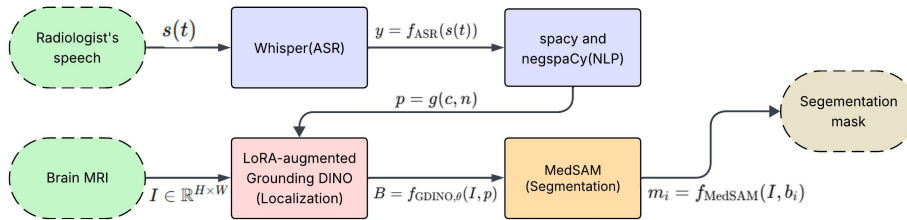


**Fig. 1. Overview of the proposed speech-guided detection-to-segmentation pipeline for brain tumor analysis.** The speech signal  $s(t)$  is transcribed and translated using Whisper [3] ASR to obtain an English transcript  $y = f_{\text{ASR}}(s(t))$ . The transcript is processed by spaCy [19] + negspaCy [18] to extract a tumor class cue and negation information, which are converted into a text prompt  $p = g(c, n)$ . In parallel, the T1-weighted brain MRI  $I \in \mathbb{R}^{H \times W}$  is provided to a LoRA-augmented GDINO localizer, which combines  $I$  and  $p$  to predict bounding boxes  $B = f_{\text{GDINO}, \theta}(I, p)$ . Each predicted box  $b_i \in B$  is then used as a prompt for MedSAM to generate a pixel-wise mask, yielding the final tumor segmentation output.

where,  $f_{\text{ASR}}$  of whisper model converts the audio signal into a transcribed text sequence  $y$  after translation into English. The reported German transcription WER of this model is 5.7% [3], while the NLP module spaCy attains 92.6% accuracy for entity extraction [19]. This clinical NLP module,  $f_{\text{NLP}}$  extracts tumor-specific semantic information, producing a candidate tumor class label  $c$  and a corresponding negation indicator  $n$ . Finally, the mapping function  $g$  generates a structured textual prompt  $p$  used to condition the downstream grounding model. The class space is defined by a controlled vocabulary dictionary,

$$\mathcal{C} = \{glioma, meningioma, pituitary, healthy\}.$$

To increase recall of tumor mentions, we use a manually curated synonym dictionary that maps each target class to a list of synonymous surface forms (e.g., *glioblastoma*  $\rightarrow$  *glioma*). This ensures that clinically relevant findings are normalized as consistent entity representations. If no tumor entity is detected, the prediction defaults to *healthy*. In addition, to reduce false-positive prompts, we perform a two-stage negation analysis. We first detect high-precision global negative cues (e.g., “no evidence of tumor” or “normal MRI”), in which case all tumor entities are treated as negated. Otherwise, entity-level negation is applied using NegEx-style trigger-and-scope rules, assigning a negation attribute  $n$  to each extracted entity.

**LoRA-augmented GDINO:** We adopt and expand the official GDINO implementation [1] with a Swin-T backbone pretrained on ImageNet. The detection module  $f_{\text{GDINO}, \theta}(I, p)$ , serves a text-conditioned tumor localizer, where  $I$  is the input MRI slice and  $p$  is the structured tumor prompt generated from radiologist dictation using the *BERT-base-uncased* text encoder of 110 million parameters. The tumor classes are manually added into the text encoder to generate

domain-specific prompt embeddings that GDINO can align with tumor regions. Additionally, we inject LoRA modules into selected attention and feed-forward layers for parameter-efficient MRI adaptation. Thus, low-rank update matrices are trained via parameters  $\theta$ , while most model parameters remain frozen. Specifically, LoRA modules are inserted into: (i) deformable self-attention layers in the encoder and decoder, (ii) vision–language cross-attention layers, (iii) feed-forward networks within transformer blocks, (iv) the initial layers of the bounding-box prediction head, (v) the feature enhancement module, and (vi) the final layers of the BERT text encoder. This targeted adaptation strategy allows the model to refine both intra-modal and cross-modal representations for MRI-specific tumor localization while maintaining parameter efficiency.

**MedSAM Segmentation:** GDINO’s predicted bounding boxes are used as prompts for MedSAM. Given an input image  $I$ , the LoRA-augmented localizer produces a set of candidate boxes

$$B = f_{\text{GDINO},\theta}(I, p) = \{(b_i, s_i)\}_{i=1}^N, \quad (1)$$

where  $b_i$  denotes the  $i$ -th bounding box and  $s_i$  its confidence score. To suppress low-confidence predictions, we apply score-thresholding and retain

$$B_\tau = \{b_i \mid s_i \geq \tau\}, \quad (2)$$

where  $\tau$  denotes the confidence threshold. MedSAM is then used in inference mode with frozen weights and leverages its pretrained medical knowledge to produce a pixel-wise segmentation for each retained box:

$$m_i = f_{\text{MedSAM}}(I, b_i), \quad b_i \in B_\tau, \quad (3)$$

where  $m_i \in \{0, 1\}^{H \times W}$  denotes the predicted tumor/background mask. The final output of LoGSAM consists of the set of masks  $\{m_i\}_{b_i \in B_\tau}$ .

**Implementation Details:** Radiologist dictations are transcribed using pretrained Whisper (large-v3) [3]. Tumor entities and negations are extracted using spaCy [19] and negspaCy [18] with a curated vocabulary. For localization, we use the official MMDetection [10] for full fine-tuning and expand the official implementation of GDINO [1] for LoRA augmentation with a Swin-T backbone and default hyperparameters. All experiments are implemented in PyTorch and run on NVIDIA A100 GPU, equipped with 40GB of RAM. LoRA modules (rank  $r = 64$ ) are injected as described in Sec. 2.2, and the model is trained on BRISC 2025 bounding-box annotations for 125 epochs using AdamW ( $2 \times 10^{-4}$ ) with a OneCycle schedule of 10% warmup and gradient clipping with a maximum norm of 5.0. For inference, given an MRI slice  $I$  and text prompt  $p$ , this pretrained LoRA-augmented GDINO (*Swin-T*) localizer predicts bounding boxes, and detections are filtered with a confidence threshold  $\tau = 0.3$ . MedSAM (ViT-B) [4], pretrained on medical datasets, is used in frozen inference mode on these predicted bounding boxes to produce the segmentation masks.

### 3 Results

We evaluate our LoGSAM pipeline performance in two stages: (i) qualitative evaluation of the class extraction model and (ii) detection-to-segmentation performance.

**Speech-to-prompt generation module:** Qualitative evaluation (Table 1) demonstrates correct prompt generation in 5 of 6 sample cases; one failure (case gg(227)) resulted from a transcription error (“glioblastoma” misrecognized as “glioplaston”). Performance is robust when tumor mentions are explicit and covered by the curated synonym list. The combined global negation detection and negspaCy gating mechanism reduces false-positive prompts. Persisting transcripts and extracted spans further enhances interpretability and debugging.

**Table 1.** Sample outputs of the Whisper and spaCy + negspaCy prompt-extraction stage on BRISC 2025 test cases, showing each case ID, the predicted class, and the transcript phrase (“evidence”) used to assign the class (including negation-based healthy cases).

Case_id	Class	Evidence
brisc2025_test_00013_gl_ax_t1	glioma	glioblastoma
brisc2025_test_00430_me_co_t1	meningioma	meningioma
brisc2025_test_00647_no_co_t1	healthy	no target tumor term found
brisc2025_test_00686_no_sa_t1	healthy	no evidence of diffusion
brisc2025_test_00743_pi_ax_t1	pituitary	macroadenoma
gg (227) (failure case)	healthy	glioplaston

**Detection-to-Segmentation Pipeline:** Table 2 shows that baseline GDINO performs strongly on BRISC in-distribution. LoRA adaptation introduces a modest reduction of 2.17% and 3.90% in mAP and mean IoU, indicating preserved localization quality. On the BBOX benchmark, detection-specific models such as YOLOv11 achieve higher raw mAP [9]; however, they rely on fixed supervision and lack text-conditioned grounding capability. In contrast, GDINO enables phrase-level localization required for speech-driven prompting. Under OOD evaluation, performance remains robust, with LoRA showing only a moderate decrease relative to the fully fine-tuned baseline.

Table 3 shows that LoGSAM achieves strong segmentation performance on BRISC 2025 without requiring manual bounding boxes at inference. The baseline fully fine-tuned GDINO + MedSAM (baseline) attains a new SOTA with mean Dice of 0.8145, while LoGSAM achieves the mean Dice score of 0.8032 (98.61% of the baseline), indicating that MedSAM remains robust to the modest drop in localization quality.

**Table 2. Detection performance of GDINO with and without LoRA augmentation under in-distribution and out-of-distribution (OOD) settings:** On BRISC dataset, LoRA augmentation achieves 97.44% of fully fine-tuned performance with only 4.96% training parameters.

Dataset	Model	mAP@50	Mean IoU
BRISC in-distribution	Baseline GDINO [10]	0.8499	0.9021
	LoRA-augmented GDINO	0.8282	0.8631
BBOX in-distribution	YOLOv11 + novel modules[9]	0.9580	-
BBOX in-distribution	Baseline GDINO [10]	0.8816	0.9004
BBOX OOD	Baseline GDINO [10]	0.8428	0.8409
	LoRA-augmented GDINO	0.7955	0.8239

**Table 3.** Segmentation performance on BRISC dataset of the proposed LoGSAM compared to current SOTA and fully fine-tuned pipeline.

Pipeline	Mean Dice Score
Trust-Refined U-Net Ensemble [16]	0.7980
Fully fine-tuned GDINO + MedSAM	0.8145
LoGSAM	<b>0.8032</b>

**Qualitative Assessment:** Fig. 2 presents qualitative results for glioma, meningioma, and pituitary tumor cases. For healthy MRIs, no segmentation is shown since the detection head identifies the entire brain region. The LoRA-augmented GDINO localizer accurately identifies tumor regions using text prompts, including challenging cases with low contrast or irregular boundaries. The resulting MedSAM masks closely align with ground-truth annotations, particularly in well-defined enhancing tumor cores. Overall, the visual results demonstrate clinically meaningful segmentation quality.

**Ablation Study:** The ablation study reveals that moderate LoRA ranks provide the best trade-off between capacity and generalization. Performance improves from  $r = 32$  to  $r = 64$ , where the model achieves its highest localization accuracy with only 4.96% trainable parameters. Further increasing the rank to  $r = 128$  degrades performance, suggesting overfitting. Similarly, adapting both visual and cross-modal components yields stronger results than modifying visual layers alone. These findings indicate that selective, low-rank adaptation is sufficient for effective MRI-specific grounding.

LoRA-based adaptation updates fewer than 5% of model parameters, introducing only a modest mAP reduction while preserving stable IoU and reliable box placement. These boxes are sufficiently accurate to guide MedSAM without requiring pixel-level supervision during training. Furthermore, performance remains robust under out-of-distribution evaluation, supporting the practicality of parameter-efficient, text-driven segmentation.

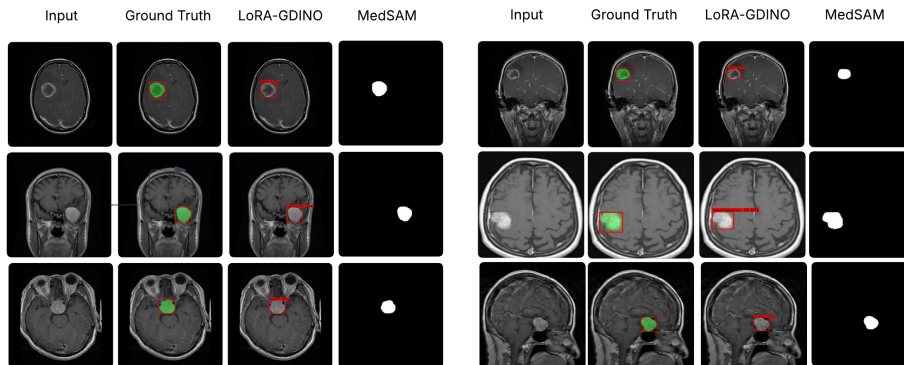


**Fig. 2. Qualitative results at different stages of the proposed detection-segmentation pipeline for two samples of each of the three tumor types.** Each row shows two representative cases: glioma (top), meningioma (middle), and pituitary tumor (bottom).

**Table 4. LoRA ablation on GDINO fine-tuning.** Reports the effect of LoRA rank size (32, 64, 128) and LoRA injection location at rank=64 on the trainable parameters and detection performance.

LoRA Rank	Params (%)	mAP@50	mIoU
$r = 32$	2.54%	0.7963	0.8614
$r = 64$	4.96%	<b>0.8282</b>	<b>0.8631</b>
$r = 128$	9.44%	0.7804	0.8257
LoRA Injection Location	Params (%)	mAP@50	mIoU
Visual Encoder + Decoder	3.71%	0.7881	0.8108
Visual Encoder + Decoder + Feature Enhancer	3.74%	0.7966	0.8627
LoGSAM (Ours)	4.96%	<b>0.8282</b>	<b>0.8631</b>

## 4 Conclusion

In this work, we demonstrate that LoGSAM effectively leverages pretrained foundation models to perform brain tumor localization and segmentation from radiologist speech cues with minimal task-specific fine-tuning. By integrating speech recognition, clinical NLP, vision-language grounding, and prompt-based segmentation into a unified pipeline, our approach enables end-to-end tumor analysis while keeping 95% of the parameters frozen. The proposed modular framework reduces dependence on densely annotated datasets and illustrates how foundation models can be intelligently coordinated to build scalable medical imaging systems. Future work will extend the framework to 3D detection and segmentation, incorporate multiple MRI sequences, and conduct broader clinical validation across diverse patient cohorts.

## References

1. Liu, S., Zeng, Z., Ren, T., et al.: Grounding DINO: Marrying DINO with Grounded Pre-Training for Open-Set Object Detection. In: European Conference on Computer Vision (ECCV), pp. 38–55. Springer, Heidelberg (2024)
2. Ronneberger, O., Fischer, P., Brox, T.: U-Net: Convolutional Networks for Biomedical Image Segmentation. In: Medical Image Computing and Computer-Assisted Intervention (MICCAI), pp. 234–241 (2015)
3. Radford, A., Kim, J. W., Xu, T., Brockman, G., McLeavey, C., Sutskever, I.: Robust Speech Recognition via Large-Scale Weak Supervision. In: Int. Conference on Machine Learning (ICML), pp. 28492–28518. PMLR (2023)
4. Ma, J., He, Y., Li, F., Han, L., You, C., Wang, B.: Segment anything in medical images. *Nature Communications*, **15**(1), 654 (2024)
5. Rasaei, H., Koleilat, T., Rivaz, H.: Grounding DINO-US-SAM: Text-Prompted Multi-Organ Segmentation in Ultrasound with LoRA-Tuned Vision-Language Models. *IEEE Transactions on Ultrasonics, Ferroelectrics, and Frequency Control* (2025)
6. Hu, E. J., Shen, Y., Wallis, P., Allen-Zhu, Z., Li, Y., Wang, S., Wang, L., Chen, W.: LoRA: Low-rank adaptation of large language models. In: International Conference on Learning Representations (ICLR), **1**(2), 3 (2022)
7. Louis, D. N., Perry, A., Reifenberger, G., et al.: The 2016 World Health Organization Classification of Tumors of the Central Nervous System. *Acta Neuropathologica* **131**(6), 803–820 (2016)
8. Bauer, S., Wiest, R., Nolte, L.-P., Reyes, M.: A Survey of MRI-Based Medical Image Analysis for Brain Tumor Studies. *Physics in Medicine & Biology* **58**(13), R97 (2013)
9. Han, W., Dong, X., Wang, G., Ding, Y., Yang, A.: Application and improvement of YOLO11 for brain tumor detection in medical images. *Frontiers in Oncology* **15**, 1643208 (2025)
10. Chen, K., Wang, J., Pang, J., Cao, Y., Xiong, Y., Li, X., Sun, S., Feng, W., Liu, Z., Xu, J., Zhang, Z.: MMDetection: Open mmlab detection toolbox and benchmark. arXiv preprint arXiv:1906.07155 (2019)
11. Jörg, T., Kämpgen, B., Feiler, D., Müller, L., Düber, C., Mildenerger, P., Jungmann, F.: Efficient structured reporting in radiology using an intelligent dialogue system based on speech recognition and natural language processing. *Insights into Imaging* **14**(1), 47 (2023)
12. Hu, J., Xu, X., Zou, Z.: LoRA-MedSAM: Efficient medical image segmentation. In: International Conference on Medical Imaging and Computer-Aided Diagnosis, pp. 154–164. Springer, Singapore (2024)
13. Chang, E. L., et al.: Radiotherapy Planning and Evaluation. *Neurosurgery Clinics of North America* **18**(1), 43–53 (2007)
14. Zhang, Y., Jiang, H., Miura, Y., Manning, C. D., Langlotz, C. P.: Contrastive learning of medical visual representations from paired images and text. In: Machine Learning for Healthcare Conference, pp. 2–25. PMLR (2022)
15. Wang, Z., Wu, Z., Agarwal, D., Sun, J.: MedCLIP: Contrastive learning from unpaired medical images and text. In: Proceedings of the Conference on Empirical Methods in NLP (EMNLP), vol. 2022, p. 3876 (2022)
16. Bhamboo, A. K., Mahala, S., Kumar, Y., Shekhawat, N. S., Sharma, K.: Trust-Refined U-Net Ensemble for Uncertainty-Aware Brain Tumor Segmentation. *Au-thorea Preprints* (2025)

17. Kirillov, A., Mintun, E., Ravi, N., Mao, H., Rolland, C., Gustafson, L., Xiao, T., Whitehead, S., Berg, A. C., Lo, W.-Y., Dollár, P.: Segment Anything. In: Proceedings of the IEEE/CVF Int. Conference on Computer Vision (ICCV), pp. 4015–4026 (2023)
18. Chapman, W. W., Bridewell, W., Hanbury, P., Cooper, G. F., Buchanan, B. G.: A simple algorithm for identifying negated findings and diseases in discharge summaries. *Journal of Biomedical Informatics* **34**(5), 301–310 (2001)
19. Honnibal, M., Montani, I., Van Landeghem, S., Boyd, A.: spaCy: Industrial-Strength Natural Language Processing in Python. Zenodo (2020)
20. Fateh, A., Rezvani, Y., Moayedi, S., Rezvani, S., Fateh, F., Fateh, M., Abolghasemi, V.: BRISC: Annotated dataset for brain tumor segmentation and classification. *Scientific Data* (2026)
21. MRI for Brain Tumor with Bounding Boxes (Kaggle dataset), <https://www.kaggle.com/datasets/ahmedsorour1/mri-for-brain-tumor-with-bounding-boxes>, last accessed 2026/02/07